on metal surfaces, in order to examine differences (or similarities) between atom–molecule and surface–molecule bonds. One can exploit the analogy between alkali atoms and rare gas metastables to compute approximate potential surfaces for Penning ionization processes in Lewis bases.

An example of their application may prove useful. Hauge, Margrave, et al.[3-5] have reported infrared spectra arising from the codeposition of water molecules and metal atoms in an argon matrix. In particular, they observed shifts in the H_2O bending frequency that they attributed to formation of AOH_2 (A = Li, Na, K, Cs, Mg, Fe, Ga, In, Tl). They also suggested the existence of a linear relationship between this frequency shift, $\Delta\nu_2$, and the dissociation energy of the complex. These complexes can be characterized by the methods reported here.[34] The results are presented in Figure 4 as a plot of $\Delta\nu_2$ vs. D_e. It appears that the alkali metals plus Mg and Fe fall on a line, whereas the group 3 metals fall on a much steeper line. The first group of atoms is spherically symmetric (the small quadrupole moment of Fe is unimportant for the energetics) and interact with water chiefly through the $3a_1$ (lone pair) orbital. The group 3 atoms have in addition an *np* electron which can interact with the $1b_2$ (OH bonding) orbital. Thus it is plausible that the two types of complex have different effects on the H_2O bending vibration. The electronic interactions underlying the frequency shift require a detailed study of force constants with a larger basis set than the present one.

Another interesting application of this set of models would be the calculation of cross sections for Penning ionization processes, such as the Penning electron-energy distribution, since an approximate excited-state potential is available here and the ionic potential may be approximated in a straightforward manner. However, neither a facile method of calculating the three-dimensional autoionization width nor a simple treatment of the anisotropic scattering problem is at hand yet.

Registry No. $LiOH_2$ (aquo form), 63313-34-8; $LiOH_2$ (hydrate form), 81408-53-9; $BeOH_2$ (aquo form), 81423-16-7; $BeOH_2$ (hydrate form), 81408-54-0; BOH_2 (aquo form), 81423-15-6; BOH_2 (hydrate form), 81408-55-1; COH_2 (aquo form), 81434-73-3; COH_2 (hydrate form), 81423-13-4; $NaOH_2$ (aquo form), 63313-37-1; $NaOH_2$ (hydrate form), 81408-56-2; $MgOH_2$ (aquo form), 81408-83-5; $MgOH_2$ (hydrate form), 81408-57-3; $AlOH_2$ (aquo form), 67187-38-6; $AlOH_2$ (hydrate form), 81408-58-4.

(34) The calculations are carried out by using data from Table III and ref 31 in eq 5–7, except for Cs and Tl, for which wave functions are not available. For these cases, valence-orbital exponents and quadrupole moments are obtained by extrapolating from the lower members of their respective groups in the periodic table.

Elementary Reconstitution of the Water Splitting Light Reaction in Photosynthesis. 1. Time-Resolved Fluorescence and Electron Spin Resonance Studies of Chlorophyll *a* Dihydrate Photoreaction with Water in Nonpolar Solutions

F. K. Fong,*,† M. Kusunoki,† L. Galloway,† T. G. Matthews,† F. E. Lytle,*,† A. J. Hoff,*,‡ and F. A. Brinkman‡

Contribution from the Department of Chemistry, Purdue University, West Lafayette, Indiana 47907, and the Deparmtent of Biophysics, Huygens Laboratory, State University of Leiden, Leiden, The Netherlands. *Received October 14, 1981*

Abstract: The path of $(Chl\ a{\cdot}2H_2O)_n$ hydrated chlorophyll *a* in its photoreaction with water is studied by means of time-resolved fluorescence and electron spin resonance techniques. It is shown that the observed ESR effects are primarily attributable to the weakly fluorescent aggregates of chlorophyll *a* dihydrate, $(Chl\ a{\cdot}2H_2O)_{n\geq 2}$. By contrast, monomeric chlorophyll *a* hydrate in nonpolar solutions containing an excess of water is photochemically inactive and instead gives rise to comparatively strong fluorescence as well as delayed fluorescence characterized by oscillatory behavior, indicative of a charge-transfer feedback mechanism. The observation of reversible, light-induced ESR signals of aggregated radical cations, $(Chl\ a{\cdot}2H_2O)_{n\geq 2}^{+\cdot}$, in the 10^{-1}–10-s domain, five decades in time removed from the oscillatory process of monomeric chlorophyll *a* hydrate suggests the critical dependence of Chl *a* photochemical properties on the state of molecular aggregation. Evidence is obtained for the aggregation of hydrated Chl *a* as the dimer, $(Chl\ a{\cdot}2H_2O)_2$, and multiples of the hexamer, $(Chl\ a{\cdot}2H_2O)_6$. The conversion of light into electrochemical potential is quantified by a weak coupling limit treatment of nonadiabatic electron transfer in terms of measured effects of ESR lifetime lengthening and line-width narrowing. The observed differences in the optical and photocatalytic properties of $(Chl\ a{\cdot}H_2O)_2$, $(Chl\ a{\cdot}2H_2O)_{n\geq 2}$, monomeric hydrated Chl *a*, and Chl *a* not complexed with water provide the rationale for proposing different stereospecific Chl *a*–H_2O aggregates as models to account for the dramatic differences in the properties of P680, P700, and light-harvesting chlorophyll associated with P680.

The storage of solar energy as fuel for the living world results from the water splitting reaction in plant photosynthesis in which oxygen is evolved and the hydrogen from water reduces carbon dioxide to carbohydrates. The mechanisms underlying this reaction may be interpreted in terms of the structural constituency of the chlorophyll *a* (Chl *a*) molecule, a pheophytin in which the hydrogen atoms at the center of the macrocycle are replaced by a Mg atom.[1] The electrophilic Mg atom and the nucleophilic cyclopentanone ring, which contains the two carbonyl groups at C9 and C10, provide the sites for molecular aggregation involving protic solvent molecules, such as water. Interactions involving the asymmetric carbon at C10 give rise to stereospecific adducts

† Purdue University.
‡ State University of Leiden.

(1) L. P. Vernon and G. R. Seely, eds., "The Chlorophylls", Academic Press, New York, 1966.

0002-7863/82/1504-2759$01.25/0

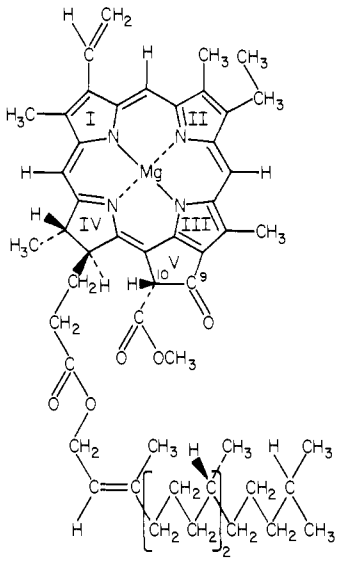

distinguished by characteristic spectroscopic and photochemical properties.[2] The different states of Chl *a* aggregation or complexation are manifested by variable red absorption maxima spanning the 670–743-nm wavelength region and by marked differences in the photoreactivity of the chlorophyll. For example, antenna chlorophylls, which display an absorption maximum of 670 nm, are photochemically inactive. Their function is to capture sunlight and transmit the photoexcitation to the reaction-center Chl *a* complexes, P680 and P700, so called on account of their red absorption maxima at 680 and 700 nm. The P680 and P700 are respectively supposed to be responsible for the evolution of molecular oxygen from water oxidation and for raising the free energy of CO_2, in the presence of light and water, to that of carbohydrates. The goal in modeling plant photosynthesis is to delineate the properties of Chl *a* aggregates in vitro and compare them to those attributed to reaction-center Chl *a* complexes in vivo. Recent work in several laboratories has focused on the modeling of P680 and P700 based on the properties of Chl *a* interactions with water in which the water oxygen atom is coordinated to the Mg atom and the two carbonyl groups of the β-keto ester function may be variously hydrogen bonded to the Mg-bound water to form different Chl *a*–H_2O aggregates.[2-12] The purpose of this work is to examine the conditions under which the in vivo phenomenon of carbon reduction by water may be reproduced in a biomimetic approach to photosynthesis research.

The P680 and P700 reaction-center Chl *a* complexes are, respectively, noted for their high and low reduction potentials, viz., ~1.0 (in excess of the 0.82-V potential needed for the O_2/H_2O redox couple at pH 7) and 0.48 V.[13] One objective of this work is to identify in vitro Chl *a* complexes possessing redox properties compatible with those of P680 and P700. In photosynthesis the light reactions of P680 and P700 make possible two vital functions in plant physiology: (1) energy storage through the reduction of CO_2 by H_2O to yield organic fuels and (2) photophosphorylation, the photoconversion of adenosine diphosphate (ADP) to the triphosphate (ATP), for satisfying the energy requirements of biosynthesis and reversal of biological cycles. The latter function is reasonably understood in terms of ADP → ATP conversion resulting from electron flow between P680 and P700 and from cyclic paths about the P680 and P700 light reactions.[14] The relationship between carbon reduction and water oxidation as a result of Chl *a* photoreaction, on the other hand, has posed difficult problems because of unresolved questions concerning Chl *a* photomechanisms relevant to the water splitting reaction. These problems are complicated by the fact that, in plant photosynthesis, carbon reduction and water splitting are mediated by enzymatic reactions that are not well understood. For example, the evolution of oxygen is assisted by manganese in a stepwise storage mechanism for the four-electron water oxidation reaction,[15] whereas carbon reduction occurs via the carboxylase reaction, made possible by the production of ribulose diphosphate (RuDP) from phosphoglyceric acid (PGA).[16] In the in vitro demonstration of the Chl *a* water splitting and CO_2 reduction reactions, Pt was employed as catalyst for the formation of reaction products.[17,18] In order to provide a starting point in establishing the in vitro behavior for contrast and comparison with the complex in vivo phenomena, it seems worthwhile to investigate initially the intrinsic properties of Chl *a* photoreaction with water in the absence of biological enzymes and/or added nonbiological catalysts. For this reason an emphasis is placed in the present study on the physical and photochemical properties of Chl *a*–H_2O aggregation in inert solvents.

Outside of the in vivo environment the chlorophyll is readily obtained as the 743-nm absorbing aggregate, (Chl *a*·$2H_2O$)$_n$.[9,10] The hydration stoichiometry of (Chl *a*·$2H_2O$)$_n$, first proposed by Holt and Jacobs,[9] was more recently established by Brace et al. using X-ray photoelectron spectroscopic techniques.[10] The structure of (Chl *a*·$2H_2O$)$_n$ was derived from the X-ray diffraction studies of Chow et al.[11] and Kratz and Duntz on ethyl chlorophyllide single crystals.[12] The dehydration of (Chl *a*·$2H_2O$)$_n$ yields the monohydrate Chl *a*·H_2O in which the water oxygen atom is coordinated to the Chl *a* Mg atom.[10] The hydration state of the chlorophyll influences the structural symmetry of Chl *a* aggregation,[2] which in turn governs the photophysical and photochemical properties of the hydrated Chl *a* adducts. For example, the C_2 symmetry of (Chl *a*·H_2O)$_2$ gives rise to specialized selection rules to the photophysical relaxation of (Chl *a*·H_2O)$_2$.[19] The photochemical response of Chl *a* films on Pt is enhanced by conversion of the chlorophyll to (Chl *a*·$2H_2O$)$_n$.[20]

The presence of molecular oxygen is of importance in Chl *a* photochemistry in vitro. In 1961 Kholmogorov and Terenin[21] showed that the illumination of solid Chl *a* in the presence of oxygen and water results in the appearance of an ESR signal. Similar results were reported by Sherman and Fujimori.[22] This signal persisted in the dark, having a width of about 1.5 G and

(2) F. K. Fong, V. J. Koester, and L. Galloway, *J. Am. Chem. Soc.*, **99**, 2372 (1977).
(3) H. Levanon and J. R. Norris, *Chem. Rev.*, **78**, 185 (1978).
(4) F. K. Fong, *Proc. Natl. Acad. Sci. U.S.A.*, **71**, 3692 (1974).
(5) L. L. Shipman, T. M. Cotton, J. R. Norris, and J. J. Katz, *Proc. Natl. Acad. Sci. U.S.A.*, **73**, 1791 (1976).
(6) S. G. Boxer and G. L. Closs, *J. Am. Chem. Soc.*, **98**, 5406 (1976).
(7) F. K. Fong, J. S. Polles, L. Galloway, and D. R. Fruge, *J. Am. Chem. Soc.*, **99**, 5802 (1977).
(8) F. K. Fong, in "Light Path of Photosynthesis", F. K. Fong, Ed., Springer-Verlag, Heidelburg, West Germany, 1982; Chapter 8.
(9) A. S. Holt and E. E. Jacobs, *Am. J. Bot.*, **41**, 710 (1954).
(10) J. G. Brace, F. K. Fong, D. H. Karweik, V. Koester, A. Shepard, and N. Winograd, *J. Am. Chem Soc.*, **100**, 5203 (1978).
(11) H. C. Chow, R. Serlin, and C. E. Strouse, *J. Am. Chem. Soc.*, **97**, 7230 (1975).
(12) C. Kratz and D. Duntz, *J. Mol. Biol.*, **113**, 431 (1977).
(13) B. Kok, B. Forbush, and M. McGloin, *Photochem. Photobiol.*, **11**, 457 (1970).
(14) D. I. Arnon, H. Y. Tsujimoto, and B. D. McSwain, *Proc. Natl. Acad. Sci. U.S.A.*, **51**, 1274 (1964).
(15) T. Wydrzynski, N. Zumbulyadis, P. G. Schmidt, H. S. Gutowsky, and Govindjee, *Proc. Natl. Acad. Sci. U.S.A.*, **73**, 1196 (1976); M. Kusunoki, K. Kitaura, K. Morokuma, and C. Nagata, *FEBS Lett.*, **117**, 179 (1980); P. Joliot, G. Barbieri, and R. Chabaud, *Photochem. Photobiol.*, **10**, 309 (1969); B. Kok, B. Forbush, and M. McGloin, *ibid.*, **11**, 457 (1970); C. F. Fowler, *Biochem. Biophys. Acta*, **462**, 414 (1977); S. Saphon, and A. R. Crofts, *Z. Naturforsch, C*, **32**, 617 (1977).
(16) J. A. Bassham and M. Calvin, "The Path of Carbon in Photosynthesis", Prentice-Hall, Englewood Cliffs, NJ, 1957, pp 51–55.
(17) F. K. Fong and L. Galloway, *J. Am. Chem. Soc.*, **100**, 3594 (1978); L. Galloway, D. R. Fruge, G. M. Haley, A. B. Coddington, and F. K. Fong, *ibid.*, **101**, 299 (1979).
(18) D. R. Fruge, G. D. Fong, and F. K. Fong, *J. Am. Chem. Soc.*, **101**, 3694 (1979).
(19) K. F. Freed, *J. Am. Chem. Soc.*, **102**, 3130 (1980).
(20) A. K. Putzeiko in "Elementary Photoprocesses in Molecules", Bertol'd S. Neporent, Ed., Nauka Press, Moscow, 1966. Translated from Russian, Consultant Bureau, New York, 1968, pp 281–299.
(21) V. E. Kholmogorov and A. N. Terenin, *Dokl. Akad. Nauk S.S.S.R.*, **137**, 199 (1961).
(22) G. Sherman and E. Fujimori, *Nature (London)*, **219**, 375 (1968).

g value of 2.005 ± 0.0003. These results suggest that (Chl $a \cdot 2H_2O)_n$, on photooxidation by O_2, is not readily regenerated in the reduced state when oxygen is present. The chemisorption of oxygen by the chlorophyll was discussed by Rosenberg and Camiscoli.[23] Deoxygenated samples were employed in the study of Chl a water splitting and carbon reduction in vitro.[17,18]

It is commonly recognized that Chl a photocatalyzes green plant photosynthesis through a one-electron transfer mechanism. Photoinduced electron spin resonance (ESR) signals were observed in photosynthetic whole cells and chloroplast preparations. A reversible ESR signal, known as signal I, was found to have the free electron g value of 2.0025 and a peak-to-peak width of about 7.5 G. In 1971 Norris et al.[28] noted that the width of the ESR signal is narrowed by a factor of $n^{-1/2}$ when an unpaired electron is spread over n Chl a molecules. On comparison of the ESR line width for the monomeric Chl a radical ion[29] in vitro with that of the P700 radical cation in vivo, these authors observed[28] a narrowing of the latter relative to the former by a factor of $2^{-1/2}$. The dimeric origin of P700 was suggested, providing the basis for proposing (Chl $a \cdot H_2O)_2$ as a plausible model for P700,[4-6] although the possible involvement[4] of an enol form of $P700^+$ was not taken into considerations of the ESR line-width narrowing. In 1975 Van Gorkum et al. reported[30] a photoinduced ESR signal which they attributed to P680. The observation[31] of reversible photoinduced ESR signals of (Chl $a \cdot 2H_2O)_{n\geq 2}^+$ in deoxygenated, wet nonpolar solutions led to the conclusion that (Chl $a \cdot 2H_2O)_{n\geq 2}$ in an O_2-depleted environment is reversibly photooxidized and dark reduced by the water. Water splitting[17] and CO_2 reduction[18] reactions were subsequently demonstrated by using (Chl $a \cdot 2H_2O)_n$ multilayers deposited on Pt foils as photocatalyst.

Our investigation of photosynthesis in vitro has continued to be concerned with the redox properties and photo properties of the monohydrate dimer, (Chl $a \cdot H_2O)_2$, and polycrystalline chlorophyll dihydrate, (Chl $a \cdot 2H_2O)_n$. The good agreement between the spectroscopic and redox properties of the former with those of P700 supports its viability as a model for P700.[8] The latter was found to be capable of photocatalyzing water splitting[17] and CO_2 reduction,[18] consistent with the model suggested for P680.[7,8] The enzymatic paths for oxygen evolution and hydrogen atom transfer in carbon reduction in vivo are replaced, for simplicity, by catalytic reaction pathways on Pt surfaces in the biomimetic approach.[17,18] The photochemical properties of the chlorophyll, in the absence and presence of the metal catalyst, and the effect of molecular oxygen on Chl a–H_2O photochemistry are examined in papers 1–3 of this series. In paper 4 the relevance of these properties to plant photosynthesis is investigated in connection with the experimental behavior of Chl a light reactions in vivo. In paper 5, the question of pheophytin and ferredoxin as intermediaries in the photosynthetic reaction is examined. The goal is to explore in vitro means for converting and storing sunlight by the Chl a water splitting and carbon reduction reactions, an in vitro reconstitution of the photosynthesis reaction making use of constituents of the in vivo apparatus.

In this paper we are concerned with the path of hydrated Chl a in its photoreaction with water. Electron spin resonance techniques are employed to quantify the kinetic behavior of the photoproduction and dark decay of (Chl $a \cdot 2H_2O)_n^+ \cdot$ in nonpolar solutions containing measured quantities of H_2O. The observed rates, monitored by the respective growth and decay of the ESR signals of (Chl $a \cdot 2H_2O)_n^+ \cdot$ when light is switched on and off, are related to the size of (Chl $a \cdot 2H_2O)_n$ obtained from the observed ESR line widths, providing the experimental criteria for analyzing the conversion of light into photoelectrochemical potential. The primary and secondary processes of the light reaction are explored by means of time-resolved fluorescence measurements. It has been found that the fluorescence quantum yield of (Chl $a \cdot 2H_2O)_n$ is two orders of magnitude lower than that of monomeric Chl a hydrate in nonpolar solutions containing an excess of water. Three distinct processes in the 10^{-10}–10^{-6}-s time span have been discerned in the multiphasic decay of hydrated Chl a fluorescence. They are interpreted in terms of, in addition to prompt fluorescence at 10^{-10}–10^{-9} s, the nonradiative conversion into a charge-separated state involving monomeric Chl a as electron donor and its water of hydration as electron acceptor, followed by charge recombination resulting in the observation of oscillatory delayed fluorescence at 10^{-6} s. The observation of reversible light-induced ESR signals of aggregated radical cations, (Chl $a \cdot 2H_2O)_n^+ \cdot$, in the 10^{-1}–10-s domain, five decades in time span removed from the oscillatory signal of monomeric hydrated Chl a, suggests the critical dependence of the Chl a photochemical properties on the aggregation state of the chlorophyll. The in vitro observations are compared and contrasted with the experimental behavior of P680 in plant photosynthesis.

Experimental Procedures

Chlorophyll a was prepared by extraction from fresh spinach and purified in the manner given by Brace et al.[10] The purified product was recrystallized as the (Chl $a \cdot 2H_2O)_n$ polycrystal in water-saturated n-pentane and stored in the dark at 10 °C. The purity of the product was established by absorption spectroscopy.[32] Chlorophyll monohydrate, Chl $a \cdot H_2O$, prepared as a solid in the usual manner[10,33] was dissolved in 1:1 mixtures of n-pentane and cyclohexane (or methylcyclohexane). The solvents were dried over solid Na. Known quantities of water were introduced into the rigorously dried Chl a solutions by using the procedure described by Fong and Koester.[34] All samples were deoxygenated by the freeze–pump–thaw method and sealed off under vacuum (5×10^{-6} torr).

Absorption measurements were made by using a Cary 14R spectrophotometer. The ESR measurements were carried out with a Varian E9 spectrometer equipped with a variable-temperature attachment. Chlorophyll radical cations in the ESR experiments were obtained by sample illumination with white light from a 1000-W tungsten iodide lamp. A Coherent Radiation Model 490 rhodamine B dye laser pumped by a Coherent Radiation Model 53 argon ion laser served as the fluorescence excitation source. The excitation spectra were measured on a 0.5-μm blazed grating. The sample fluorescence was chopped by a frequency-controlled motor accurate to 0.5%. The output of the photomultiplier was fed into a phase-sensitive detection system consisting of a Keithly nanovolt amplifier, a Keithly phase shifter, and a Keithly phase-sensitive detector. The resulting signal was displayed on a strip-chart recorder. A 1000-W tungsten–halogen lamp in conjunction with a 0.25-m Jarrell Ash monochromator served as the variable-wavelength source used in the recording of excitation spectra. A Laser Precision Model 3440 pyroelectric radiometer and a model RP-433 probe were employed to determine the spectral distribution of the lamp intensity for the purpose of correcting the excitation spectra.

Fluorescence lifetimes were measured by using a Phase-R Model N21K nitrogen laser system. The N_2^+ laser provided 337-nm, 3-μJ, 4.5-ns pulses at repetition rates of up to about 35 Hz. The fluorescence lifetimes of monomeric and polymeric Chl a were measured with the fluorescence monitored through a Corning 0-52 UV filter, a 2-60 red filter, and a Jarrell Ash 0.25-m monochromator. Time resolution of the prompt (<10 ns) fluorescence was achieved by a Tekronix Model 5S15N sampling oscilloscope. A PAR Model 162 Boxcar integrator was used to monitor the delayed (>50 ns) luminescence. The flux dependence measurements were accomplished by placing a series of neutral density filters in front of the N_2 laser excitation. Temperatures below room temperature were maintained by a cryostat. The temperature was varied

(23) B. Rosenberg, and J. F. Camiscoli, *J. Chem. Phys.*, **35**, 982 (1961).
(24) B. Commoner, J. Heise, and J. Townsend, *Proc. Natl. Acad. Sci. U.S.A.*, **42**, 710 (1956).
(25) P. Sogo, N. Pon, and M. Calvin, *Proc. Natl. Acad. Sci. U.S.A.*, **43**, 387 (1957).
(26) B. Commoner, J. Heise, B. Lippincott, R. Norberg, J. Passinneau, and J. Townsend, *Science (Washington, D.C.)*, **125**, 57 (1957).
(27) H. Beinert, B. Kok, and G. Hoch, *Biochim. Biophys. Res. Commun.*, 7, 209 (1962).
(28) J. R. Norris, R. A. Uphaus, H. L. Crespi, and J. J. Katz, *Proc. Natl. Acad. Sci. U.S.A.*, **68**, 625 (1971).
(29) B. D. C. Borg, J. Fajer, R. H. Felton, and D. Dolphin, *Proc. Natl. Acad. Sci. U.S.A.*, **67**, 813 (1970).
(30) H. J. Gorkum, J. J. Tamminga, and J. Haveman, *Biochem. Biophys. Acta*, **347**, 417 (1974).
(31) F. K. Fong, A. J. Hoff, and F. A. Brinkman, *J. Am. Chem. Soc.*, **100**, 619 (1978).
(32) H. H. Strain, M. R. Thomas, and J. J. Katz, *Biochem. Biophys. Acta*, **75**, 306–311 (1963).
(33) N. Winograd, A. Shepard, D. H. Karweik, V. Koester, and F. K. Fong, *J. Am. Chem. Soc.*, **98**, 2369 (1976).
(34) F. K. Fong and V. J. Koester, *Biochem. Biophys. acta*, **423**, 52 (1976).

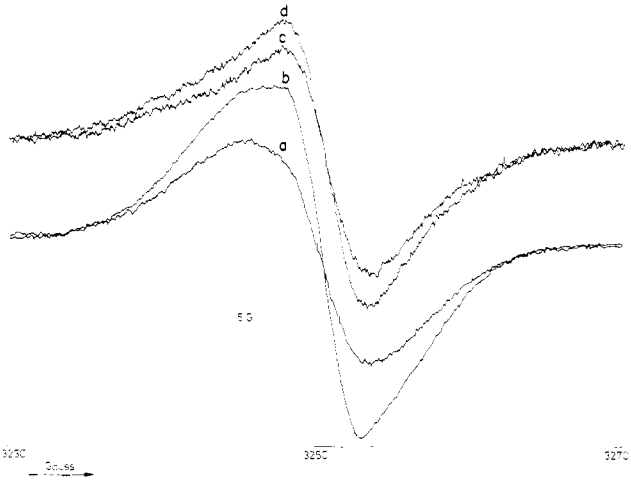

Figure 1. Light-induced ESR spectrum of hydrated Chl *a* radical cation in dry 1:1 n-pentane–cyclohexane: (a) 10 °C dark spectrum after several cycles of illumination; (b) 10 °C spectrum of sample in a under subsequent illumination by white light; (c) dark spectrum at −140 °C after several cycles of illumination; (d) spectrum of sample in c during illumination at −140 °C. The experimental conditions are given as follows: microwave power, 10 mW; modulation, 6.3 G; gain (a) 3.2×10^3, (b) 4×10^3, (c) and (d) 6.3×10^3.

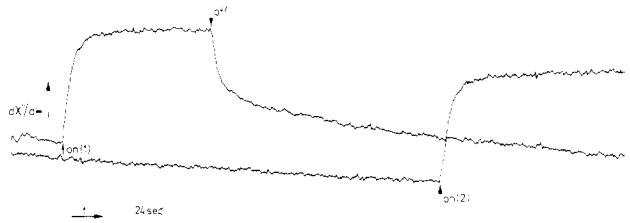

Figure 2. Kinetics of light production and dark decay of photoinduced hydrated Chl *a* radical cation in 1:1 *n*-pentane–cyclohexane at 10 °C. Absorption of microwave power was monitored at the low-field first derivative peak. The microwave power and modulation settings are the same as those given in Figure 1. The gain was 6.3×10^3. A preilluminated sample, after having been kept in the dark for 16 min, was illuminated at the first arrow, marked "on (1)". After another period of dark decay, the sample was again illuminated at the second arrow, marked "on (2)". The reproducible kinetic effects were reversible through many light–dark cycles. Complete dark decay of the photoinduced ESR signal took >1 h.

at a rate of ~30 deg h^{-1} according to the procedure of Fong and Koester.[34] Between runs the samples were kept in the dark.

Experimental Results

The ESR signals observed in a rigorously dried 10^{-4} M Chl *a* solution in 1:1 *n*-pentane–cyclohexane, in which no water was intentionally added, are shown in Figure 1. The *g* value of this signal was found to be 2.003 ± 0.001. From the decay kinetics observed after the light was turned off (see Figure 2), we note that the ESR signal consists of two components, one transient and the other long lived. It was found that the relative importance of these two components varies with the temperature. At 10 °C the signal decays within 1 s by ~20%. At −140 °C the observed ESR signal is mostly irreversible. The line shape of the 10 °C reversible signal is distinctly asymmetric. The corresponding long-lived component is nearly symmetrical (see Figure 1a). The asymmetry becomes more pronounced at lower temperatures. The microwave power saturation behavior of the −140 °C low-field shoulder is indistinguishable from that of the first-derivative peak. The line width of the ESR signal decreases with temperature, being 7.5 and 5.5 G at 10 and −140 °C, respectively (compare spectra a and b with c and d in Figure 1). The 10 °C long-lived component is approximately Gaussian in line shape. At low temperatures, the line shape becomes Lorentzian, suggestive of an increase in the exchange narrowing with decreasing temperature. At 10 °C the peak-to-peak line width of the transient signal in

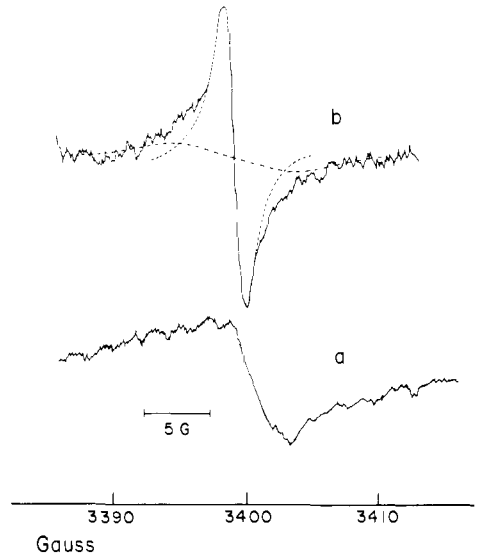

Figure 3. Light-minus-dark reversible ESR signals of $(\text{Chl } a \cdot 2H_2O)_n^{+\cdot}$ observed in 1:1 *n*-pentane–cyclohexane. (a) 4×10^{-3} M Chl *a*–2 M H_2O, the ESR signal is non-Gaussian with a peak-to-peak width of about 6.4 G indicative of the presence of at least two active aggregate species; (b) water-saturated 4×10^{-3} M Chl *a*, the ESR signal is decomposed into a weak monomeric Chl $a^{+\cdot}$ band and a narrow component (line width 1.7 G) attributed to $(\text{Chl } a \cdot 2H_2O)_{(n)\simeq 38}^{+\cdot}$. The experimental conditions are given as follows: microwave power, 10 mW; modulation, 2 G; gain (a) 1.60×10^4 and (b) 1.25×10^4.

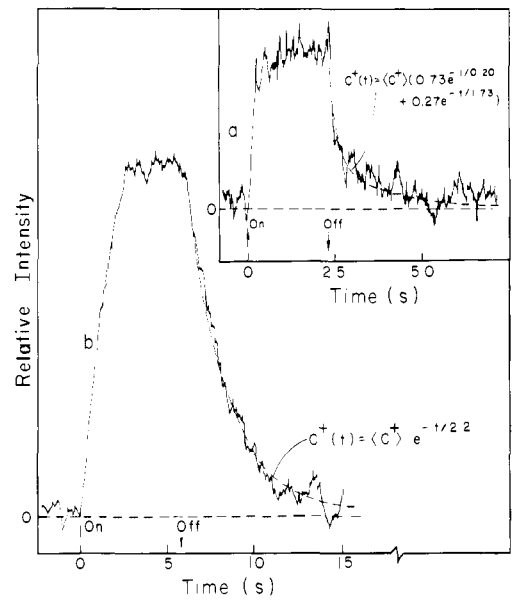

Figure 4. Kinetic behavior of the photogeneration and dark decay of the reversible ESR signals shown in (a) and (b) in Figure 3. The letter indexes a and b correspond to those in Figure 3. The microwave power and modulation settings are the same as those given in Figure 3. The gain in both a and b was 6.3×10^4. See text for a detailed discussion of the numerical fits of the experimental data.

Figure 1 narrows to 1.3 G in 3–4 days after the addition of an excess of water. The appearance of the narrow-width ESR signal is accompanied by a diminution of the irreversible ESR component.

The light-minus-dark ESR spectra of samples were recorded so as to eliminate ESR contributions from the long-lived Chl *a* radical cations. The ESR signals observed at 20 °C in 4×10^{-3} M Chl *a*–2 M H_2O and water-saturated 4×10^{-3} M Chl a solutions in 1:1 *n*-pentane–cyclohexane are shown in Figure 3. The corresponding kinetic data are shown in Figure 4.

The absorption spectra of a water-saturated 10^{-4} M Chl *a* solution in 1:1 *n*-pentane–methylcyclohexane (NP–MCH) re-

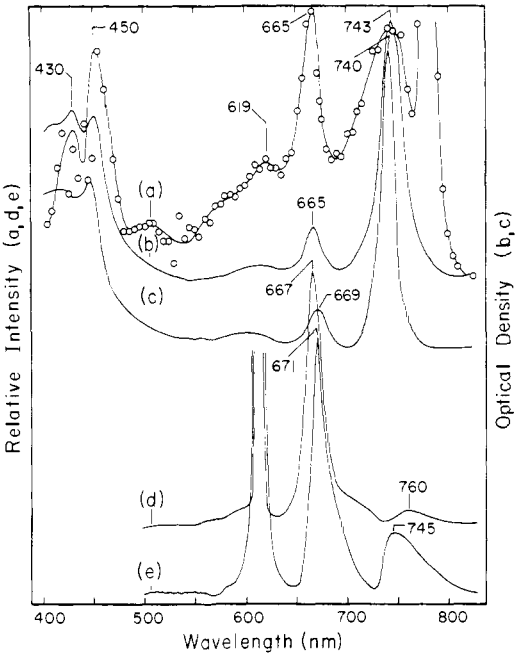

Figure 5. Absorption, fluorescence, and excitation spectra of a 10^{-4} M water-saturated Chl *a* sample prepared in a 1:1 mixture of water-saturated *n*-pentane and methylcyclohexane. (a) Room temperature (294 K) fluorescence excitation spectrum monitored at 780 nm, corrected for the spectral distribution of the excitation source; (b), (c) absorption spectra at 294 and 90 K, respectively; (d), (e) fluorescence spectra at 294 and 90 K, respectively. The fluorescence spectra, excited by an Ar-laser pumped rhodamine B dye laser (0.2 W, all lines), are uncorrected for the S-20 response of the photomultiplier tube. The absorption spectra indicate that >90% of the chlorophyll exists as the 743-nm absorbing Chl *a* dihydrate polycrystal (Chl $a{\cdot}2H_2O)_n$. The fluorescence maximum at 667 nm (671 nm) is attributable to monomeric Chl *a* present in equilibrium with the Chl *a* dihydrate polymer. The excitation spectrum indicates that the 760-nm (745 nm) fluorescence band (d), (e) has originated from (Chl $a{\cdot}2H_2O)_n$ emission.

corded at 294 and 90 K are respectively shown in Figure 5, b and c. The fluorescence spectra of the 10^{-4} M Chl *a* sample measured at 294 and 90 K are respectively shown in Figure 5, d and e, respectively. The spectra were uncorrected for the spectrometer response and the S-20 response of the photomultipler tube. At both temperatures two main fluorescence bands were obtained at 667 (671)[34-37] and 760 nm. The room temperature excitation spectrum of the 10^{-4} M Chl *a* sample (fluorescence monitored at 780 nm) is shown in Figure 5a. The intense line at 780 nm was due to the fluorescence monitor. The spectrum was corrected for the spectral distribution of the excitation source. Fluorescence decay for chlorophyll *a* emission at various temperatures are given in Figure 6. The prompt fluorescence decay was monitored at 680 and 757 nm. The decay curves for the 757- and 680-nm fluorescence at 90, 125, 250, and 294 K were fitted by computer-generated exponential convolutions[38] (Figure 6b–g) of the instrumental pulse decay (Figure 6a). The biphasic fluorescence decay for (Chl $a{\cdot}2H_2O)_n$ at 90 and 125 K were both fitted by the convolute corresponding to a lifetime, τ_f, of 0.6 ns at short time values (Figure 6c). A second decay component having an ap-

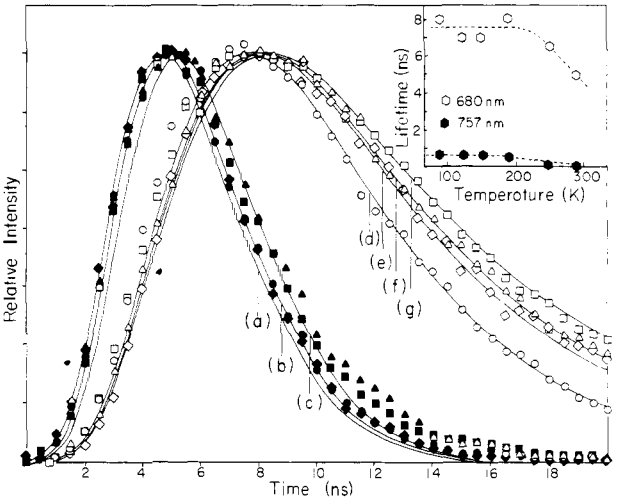

Figure 6. Temperature dependence of the prompt fluorescence decay of a 10^{-4} M Chl *a* solution prepared in a 1:1 mixture of water-saturated *n*-pentane and methylcyclohexane. The fluorescence decay was monitored at 757 (solid symbols, except where data points overlap) and 680 nm (open symbols). The lifetimes of the fluorescence decay curves at 293 K (●,○), 250 K (♦,◇), 125 K (▲,△), and 90 K (■,□) have been determined by comparison with computer-generated single-exponential convolutions of the (a) instrumental pulse; (b)–(g) sample fluorescence lifetimes 0.25, 0.60, 5.0, 6.5, 7.0, and 8.0 ns, respectively. The departure from the single-exponential fits for the 757-nm fluorescence (b), (c) at longer times, in comparison with the good agreement obtained for corresponding fits of the 680-nm fluorescence, reveals the existence of a longer decay component having an approximate lifetime of 3.5 ns. The convolutions provide a qualitative contrast of the (Chl $a{\cdot}2H_2O)_n$ fluorescence lifetimes with those of monomeric Chl *a* (d)–(g) at comparable temperatures. A check of the room-temperature result using a dye laser system capable of generating an instrumental pulse (500 ps) narrower in time than that (5 ns) of the N^{2+} laser system produced a value $\tau \lesssim 50$ ps for the (Chl $a{\cdot}2H_2O)_n$ fluorescence. The temperature dependence of the fluorescence lifetimes of (Chl $a{\cdot}2H_2O)_n$ and monomeric Chl *a* are summarized in the inset.

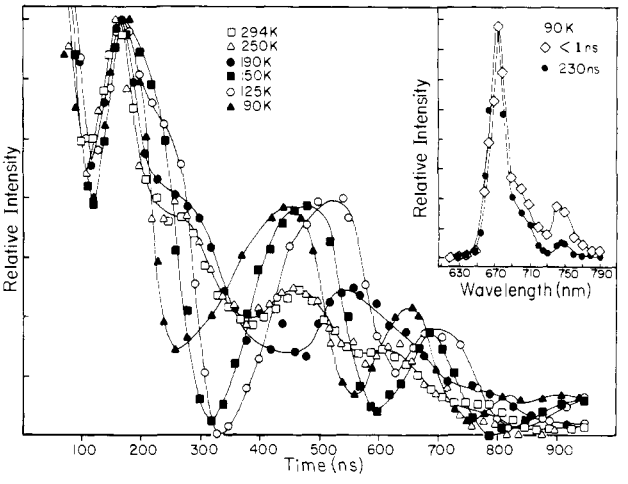

Figure 7. Temperature dependence of the delayed fluorescence decay of a 10^{-4} M Chl *a* sample prepared in a 1:1 mixture of water-saturated *n*-pentane and methylcyclohexane: (□) 294, (△) 250, (●) 190, (■) 150, (○) 125, and (▲) 90 K. The decay curves are corrected for the instrumental noise. At $T \lesssim 150$ K four maxima are reproducibly observed at $\tau < 1$ μs. No additional maxima were observed when the decay time scale is extended to 5 μs. At temperatures greater than 150 K, the maxima are dampened to give an approximately exponential decay. A comparison of the time-resolved fluorescence spectra monitored at <1 and 230 ns after excitation is shown in the inset.

proximate lifetime, τ_b, of 3.5 ns was obtained at longer times (Figure 6c). At $T \gtrsim 250$ K the short ($\lesssim$0.25 ns) fluorescence lifetimes were beyond the instrumental limit (Figure 6b). Reproduction of the 757-nm fluorescence lifetime measurement at 294 K was accomplished by using a frequency-doubled dye laser

(35) R. Livingston, "Photosynthesis in Plants", Iowa State College Press, Ames, IA, 1949; R. Livingston, W. F. Watson, J. McArdle, *J. Am. Chem. Soc.*, **71**, 1542 (1945); F. S. Forster and R. Livingston, *J. Chem. Phys.*, **20**, 1315 (1952).

(36) S. S. Brody, *Science (Washington, D. C.)*, **128**, 838 (1958); S. S. Brody, and M. Brody, *Trans. Faraday Soc.*, **58**, 416 (1962); S. S. Brody and S. B. Brody, *Biophys. J.*, **8**, 1511 (1968); C. Balny, S. S. Brody, and G. H. B. Hoa, *Photochem. Photobiol.*, **9**, 445 (1969).

(37) P. S. Stensby and J. L. Rosenberg, *J. Phys. Chem.*, **65**, 906 (1961); R. J. Marcus and G. R. Haugen, *Photochem. Photobiol.*, **4**, 183 (1965); K. Kawake, M. Maemua, and Y. Matsukawa, *Technol. Rep. Osaka Univ.*, **20**, 665 (1970); E. Vavrinec, K. Vacek, and M. Kaplanova, *J. Lumin.*, **5**, 449 (1972); M. Kaplanova and K. Vacek, *Photochem. Photobiol.*, **22**, 371 (1974).

(38) F. E. Lytle, *Photochem. Photobiol.*, **17**, 75 (1973).

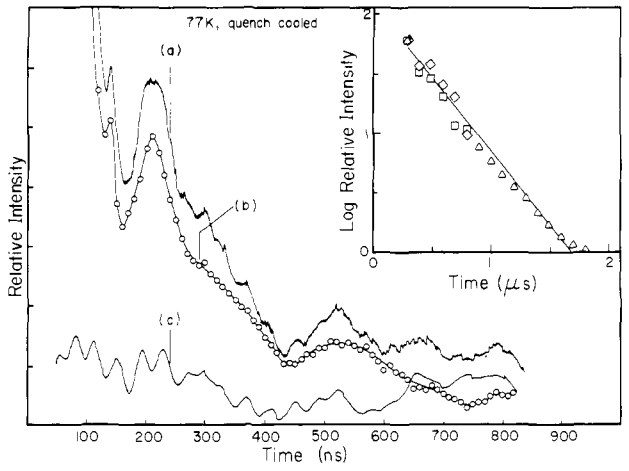

Figure 8. Effect on the delayed fluorescence decay of quench cooling the 10^{-4} M Chl *a* sample to 77 K: (a) uncorrected fluorescence decay; (b) base-line-corrected decay; (c)base line. A comparison of the room-temperature decay to the quench-cooled decay is shown in the inset: (□, △) data points obtained from 1- and 10-μs full-scale decay measurements at 77 K, respectively; (◇) data points obtained from 1-μs full-scale decay measurements at 294 K. The semilogarithmic plot in the inset indicates that the 294-K and quench-cooled (77 K) delayed fluorescence decay plots follow an approximate exponential behavior.

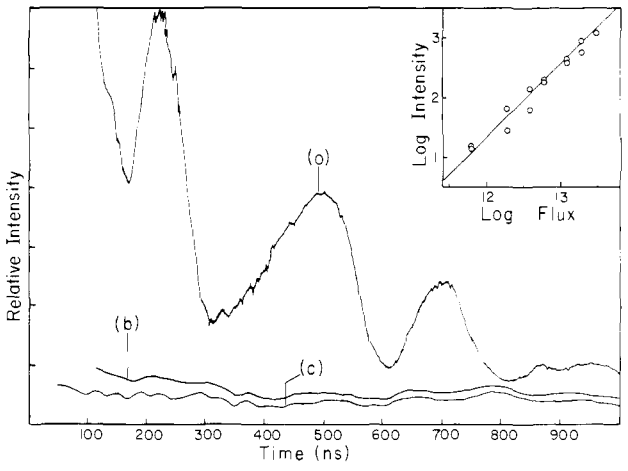

Figure 9. Comparison of the 90-K delayed fluorescence decay curves for 10^{-4} M Chl *a* solutions: (a) in a 1:1 mixture of water-saturated *n*-pentane (NP) and methylcyclohexane (MCH) and (b) in a 5:2 mixture of diethyl ether and *n*-propanol. The chlorophyll exists predominantly in the monomeric state in ether/*n*-propanol. The delayed fluorescence observed in the ether/*n*-propanol sample is barely detectable over the base line (c). The linear flux dependence of the chemiluminescence intensity monitored 230 ns after sample excitation is shown in the inset.

system capable of producing a 500-ps instrumental pulse.[39] A value of $\tau \lesssim 50$ ps was obtained in this experiment.

In addition to the short-lived (<10 ns) fluorescence observed at 680 and 757 nm, a long-lived (>100 ns) component in the fluorescence decay was observed (see Figure 7). The base-line-corrected decay of this fluorescence was found to be strongly temperature dependent, with an oscillatory structure at temperatures ≲150 K. Above 150 K the oscillatory pattern appears dampened, converging to a nearly exponential decay function. Lifetime measurements on the solvent fluorescence in the absence of Chl *a* revealed no detectable deviation from the base line. Intentional alteration of the time dependence of the base-line noise produced no change in the oscillatory structure of the sample delayed fluorescence decay. Time-resolved fluorescence spectra measured at 230 (inset, Figure 7), 400, 600, and 800 ns along the decay time coordinate show that the chlorophyll is responsible for the observed long-lived fluorescence. The delayed fluorescence spectra differ from the prompt fluorescence spectra in that monomeric hydrated Chl *a* fluorescence at 670 nm appears enhanced relative to (Chl $a{\cdot}2H_2O)_n$ fluorescence at longer wavelengths.

The delayed fluorescence decay of a sample quench cooled to liquid nitrogen temperature (Figure 8) resembles that observed at room temperature (compare Figure 8b with Figure 7). Both decay curves follow a nearly exponential behavior (inset, Figure 8), converging with the base line at times greater than 1 μs. The linear flux dependence of the delayed fluorescence intensity measured at 230 ns after laser excitation is shown in the inset of Figure 9.

In order to examine the origin of the long-lived emission, a 10^{-4} M Chl *a* sample was prepared in 5:2 mixture of diethyl ether and *n*-propanol. In nonaqueous polar solvents, Chl *a* exists predominantly in the monomeric state.[40-44] The delayed fluorescence decay at 90 K for Chl *a*/ether–propanol is compared with that for the (Chl $a{\cdot}2H_2O)_n$/NP–MCH sample in Figure 9. This comparison shows that the delayed fluorescence is predominantly a property of hydrated Chl *a* in nonpolar solvents containing an excess of water.

Discussion

The line-width narrowing of the reversible ESR signal in Figure 1 on addition of excess water, accompanied by a diminution of the irreversible ESR component, is reflected by the observed[34] growth of the 743-nm absorbing Chl *a* aggregate, (Chl $a{\cdot}2H_2O)_n$, under similar experimental conditions. The reversible signal is thus primarily attributable[31] to (Chl $a{\cdot}2H_2O)_{n>2}^{+\cdot}$.

Photocatalytic activity is predicated upon the ability of the light-induced chlorophyll radical cation to be regenerated in the neutral state in the dark. The light-minus-dark ESR signals obtained from the water-saturated sample (Figure 3b) consist of two Gaussian components. A weak line of 10.4-G width attributable to monomeric Chl $a^{+\cdot}$[29] is detected underlying the main component of 1.7-G width. From the latter width we obtain (Chl $a{\cdot}2H_2O)_{\langle n\rangle\simeq 38}^{+\cdot}$ as the predominant photocatalytic aggregate. The observed superposition of Chl $a^{+\cdot}$ and (Chl $a{\cdot}2H_2O)_n^{+\cdot}$ ESR signals suggests the existence of a dissociation equilibrium:

$$(\text{Chl } a{\cdot}2H_2O)_n^{+\cdot} \rightleftharpoons (\text{Chl } a{\cdot}2H_2O)_{n-1} + (\text{Chl } a{\cdot}2H_2O)^{+\cdot} \quad (1)$$

The decay of (Chl $a{\cdot}2H_2O)_n^{+\cdot}$ after sample illumination is thus expected to deplete the light-induced monomeric Chl $a^{+\cdot}$ through a leftward displacement of the equilibrium in 1. The interpretation of a single predominant photocatalytic species in the water-saturated sample, as given in reaction 1, is consistent with the simple exponential decay law

$$C^+(t) = \langle C^+\rangle e^{-t/2.2} \quad (2)$$

obtained from fitting the kinetic data shown in Figure 4b. Significantly, in this interpretation, there is no evidence that the monomer (Chl $a{\cdot}2H_2O)^{+\cdot}$ is a photocatalytic species. In eq 2, $\langle C^+\rangle$ and $C^+(t)$ are, respectively, the steady-state concentration under illumination and the concentration after illumination of (Chl $a{\cdot}2H_2O)_n^{+\cdot}$ in the water-saturated sample. The lifetime of (Chl $a{\cdot}2H_2O)_{\langle n\rangle\simeq 38}^{+\cdot}$ is given by $\tau_{38} = 2.2$ s.

The light-minus-dark ESR spectrum obtained from the 2 M H_2O solution (Figure 3a) is non-Gaussian, suggesting the existence of at least two active species present in comparable amounts. The peak-to-peak width is about 6.4 G, intermediate between the observed and expected widths, 7.5 and <6.1 G, for (Chl $a{\cdot}2H_2O)_2^{+\cdot}$ and (Chl $a{\cdot}2H_2O)_{n>3}^{+\cdot}$, respectively, from which we conclude that one of the ESR-active species is (Chl $a{\cdot}2H_2O)_2^{+\cdot}$. The existence of two photocatalytic aggregates in the 2 M H_2O sample is

(39) T. H. Bushaw, F. E. Lytle, and R. S. Tobias, *Appl. Spectrosc.*, **32**, 585 (1978); J. M. Harris, L. M. Gray, M. J. Pelletier, and F. E. Lytle, *Mol. Photochem.*, **8**, 161 (1977).
(40) A. N. Terenin, "Second All-Union Conference on Photosynthesis, Moscow, English Translation", Consultants Bureau, New York, 1957.
(41) R. Livingston, *Q. Rev. (London)*, **14**, 174 (1960).
(42) J. J. Katz, G. L. Closs, F. C. Pennington, M. R. Thomas, and H. H. Strain, *J. Am. Chem. Soc.*, **85**, 1301 (1963).
(43) G. L. Closs, J. J. Katz, F. C. Pennington, M. R. Thomas, and H. H. Strain, *J. Am. Chem. Soc.*, **85**, 1309 (1963).
(44) T. M. Cotton, A. D. Trifunac, K. Ballschmiter, and J. J. Katz, *Biochim. Biophys. Acta*, **368**, 181 (1974).

supported by the biphasic decay data in Figure 4a, which are numerically fitted by the expression

$$C^+(t) = \langle C^+ \rangle (0.73e^{-t/0.20} + 0.27e^{-t/1.73}) \quad (3)$$

The lifetimes of the two aggregate radical cation species are thus given by 0.20 and 1.73 s.

In the presence of a metal catalyst the (Chl $a{\cdot}2H_2O)_n^{+\cdot}$ cation reacts with water leading to oxygen evolution[17]

$$(\text{Chl } a{\cdot}2H_2O)_n^{+\cdot} + {}^1/_2\, H_2O \rightarrow (\text{Chl } a{\cdot}2H_2O)_n + H^+ + {}^1/_4\, O_2 \quad (4)$$

where water is the electron donor for (Chl $a{\cdot}2H_2O)_{n\geq 2}^{+\cdot}$. The oxygen evolution process in reaction 4 in the absence of a metal catalyst is expected to be negligibly slow. Even so electron transfer from bound water molecules to (Chl $a{\cdot}2H_2O)_{n\geq 2}^{+\cdot}$ is most likely responsible for the observed dark decay of photogenerated (Chl $a{\cdot}2H_2O)_n^{+\cdot}$. Recombination of light-induced radical cations and anions is improbable on account of their extremely small concentrations. Consider the electron-transfer process

$$(\text{Chl } a{\cdot}2H_2O)_n^{+\cdot}{\cdot}(H_2O)_n \rightarrow (\text{Chl } a{\cdot}2H_2O)_n{\cdot}(H_2O)_n^{+} \quad (5)$$

where $(H_2O)_n$ denotes the n water molecules equivalently bound to the polymeric cation, (Chl $a{\cdot}2H_2O)_n^{+\cdot}$. The inverse lifetime, τ_n^{-1}, of (Chl $a{\cdot}2H_2O)_n^{+\cdot}$ may be given according to the treatment of nonadiabatic electron transfer[45] as the sum of electron tunneling probabilities, $W_{i(n)}$, from the ith bound water molecule

$$\tau_n^{-1} = \sum_{i=1}^{n} W_{i(n)} = \sum_{i=1}^{n} |T_{i(n)}|^2 F_{i(n)} \quad (6)$$

where $F_{i(n)}$ is the Frank–Condon factor and $T_{i(n)}$ is the electron tunneling matrix element between the ith donor water molecule and (Chl $a{\cdot}2H_2O)_n^{+\cdot}$. The dependence of τ_n on the aggregate size, n, may generally be derived from $F_{i(n)}$ as well as $T_{i(n)}$ through the n-dependent redox potential, E_n^0, of (Chl $a{\cdot}2H_2O)_n^{+\cdot}$, which is related to the energy difference between the ground-state energy, $E_+(n)$, of (Chl $a{\cdot}2H_2O)_n^{+\cdot}$ and that, $E_0(n)$, of (Chl $a{\cdot}2H_2O)_n$, i.e.,

$$E_n^0 = E_+(n) - E_0(n) \quad (7)$$

The narrowing[28,31] of the (Chl $a{\cdot}2H_2O)_n^{+\cdot}$ ESR line width arises from delocalization of the positive spin over the n Chl $a{\cdot}2H_2O$ monomer units, suggesting that the n macrocycle π-electron systems of (Chl $a{\cdot}2H_2O)_n^{+\cdot}$ may be described by a box given by $L_xL_yL_z = nLa^2$, where $L_xL_y = a^2$ is the area of the Chl a macrocycle and $L_z = nL$ is the length of the macrocycle aggregate, with n donor water molecules weakly bound in a periodic arrangement along the z axis. In this case $T_{i(n)}$ may be approximately written

$$T_{i(n)} = -[E_n^0 + h^2(2a^{-2} + n^{-2}L^{-2})/8m^*]\, S_{i(n)}{}^{xy}\, S_{i(n)}{}^{z} \quad (8)$$

where h is the Plank constant, m^* is the effective mass for delocalized electron motion, $S_{i(n)}{}^{xy}$ and $S_{i(n)}{}^{z}$ are, respectively, the half-overlap integrals over the xy plane and along the z axis of the acceptor cation. The $S_{i(n)}{}^{z}$ is proportional to $n^{-1/2}$ due to normalization of the z component of the acceptor wave function. Otherwise $S_{i(n)}{}^{xy}$ and $S_{i(n)}{}^{z}$ only depend weakly on n. Significantly the $n^{-1/2}$ dependence of $S_{i(n)}{}^{z}$ is exactly canceled out by the number of water molecules contributing to the summation in eq 6, and the second term in the bracket of eq 8 is usually much smaller than the first one owing to the large effective mass, m^*. The above considerations imply that the Frank–Condon factor $F_{i(n)}$ may be sufficiently sensitive on E_n^0 as to account for the n dependence of τ_n even if E_n^0 changes by energy amounts as small as 0.1 eV corresponding to the red shifts in the absorption band with increasing n. Reaction 5 is given by the energy change, $\Delta E = E' - E_n^0$, where E' is the energy difference between H_2O^+ and H_2O. Since reaction 5 is exothermic, $F_{i(n)}$ is expected to be a decreasing function of ΔE, which in turn should increase monotonically with increasing n to be compatible with the fact that $\tau_{\langle 38 \rangle} = 2.2$ s is significantly larger than τ_2 and τ_6. Hence, we can safely assign the shorter and the longer of the two lifetimes in eq 3 to (Chl $a{\cdot}2H_2O)_2^{+\cdot}$ and (Chl $a{\cdot}2H_2O)_6^{+\cdot}$, i.e., $\tau_2 = 0.20$ s and $\tau_6 = 1.73$ s, respectively.

Using the energy gap law for $F_{i(n)}$ in the weak coupling limit[46] and taking into account the negligibly small dependence of $\sum_{i=1}^{n}|T_{i(n)}|^2$ on n, the approximate formula relating the redox potential difference, E_2^0, and the lifetime ratio (τ_n/τ_2) is obtained[46]

$$E_n^0 - E_2^0 \approx \hbar\omega_m \ln(\tau_n/\tau_2)/(\ln[(E_2^0 - \epsilon)/L_m g_m^2 \hbar\omega_m(1 + n(\hbar\omega_m))] - 1) \quad (9)$$

where the subscript m denotes the accepting mode of maximum coupling specified by frequency ω_m and the coupling strength $L_m g_m^2$, and $n(\hbar\omega_m)$ is the Bose distribution function. In arriving at eq 9 the approximate inequalities $E_2^0 \lesssim E_n^0$ are obtained. Assuming that the weighting factors 0.73 and 0.27 in eq 3 apply to the relative populations of (Chl $a{\cdot}2H_2O)_2^{+\cdot}$ and (Chl $a{\cdot}2H_2O)_6^{+\cdot}$ and employing the expected width, 4.3 G, for the (Chl $a{\cdot}2H_2O)_6^{+\cdot}$ ESR line, we estimate a narrowing of the 7.5-G line width for pure (Chl $a{\cdot}2H_2O)_2^{+\cdot}$ to an apparent width of 6.6 G for the two-component mixture given in eq 3, in agreement with the value, 6.4 G, observed in Figure 3a. The approximate multiples of 6 in (Chl $a{\cdot}2H_2O)_{\langle n \rangle \simeq 6}$ and (Chl $a{\cdot}2H_2O)_{\langle n \rangle \simeq 38}$ suggest the intriguing possibility that polymeric (Chl $a{\cdot}2H_2O)_n$ aggregates are stabilized in hexameric units.

The relative intensity of the 743-nm absorption shown in Figure 5b,c indicates that more than 90% of the chlorophyll exists as (Chl $a{\cdot}2H_2O)_n$.[10] The non-Gaussian shape of the broad 743-nm band reflects, in addition to possible non-Gaussian contributions from overlapping vibronic transitions, the inhomogeneity of the aggregate size. As the sample is slowly cooled to 90 K, below the glass-transition temperature (125 K) of the solvent mixture, this band is seen to be blue shifted to 740 nm and narrows significantly, suggesting a partial ordering of and/or an increasing uniformity in the size of the aggregates.

The fluorescence band at 667 (671) nm in Figure 5d,e appears indistinguishable from that observed previously[34-37] in nonpolar solutions of Chl a. It is attributable to monomeric Chl a fluorescence[34,35] corresponding to the 665- (669-) nm absorption band in Figure 5b,c. The intensity ratio of the 667- and 760-nm fluorescence bands is greater at room temperature than at low temperatures (compare Figure 5,d and e). The appearance of a weak fluorescence band at 720 nm reveals the presence of a small amount of hydrated Chl a dimers.[6,34] The absence of the dimer band in the 90 K spectrum suggests the aggregation of dimeric hydrated Chl a to yield polymeric (Chl $a{\cdot}2H_2O)_n$ as the temperature is lowered. From the dramatic reversal in the intensity ratios of the corresponding absorption and fluorescence bands in Figure 5, we find that the fluorescence quantum yield, η_n, of (Chl $a{\cdot}2H_2O)_n$ is approximately two orders of magnitude lower than that, η_1, of monomeric Chl a, with $\eta_n \simeq 0.02\eta_1$ and $\eta_n \simeq 0.01\eta_1$ at 90 and 294 K, respectively.

Observation of the 743-nm band suggests that the fluorescence at 760 nm is associated with (Chl $a{\cdot}2H_2O)_n$ emission. The presence in the 780-nm fluorescence excitation spectrum of a band at 665 nm provides evidence for energy transfer from Chl a monomers to the polymeric aggregates. Significantly, the intensity at 665 nm is greater than that at 743 nm in Figure 5a, in spite of the considerably weaker monomeric Chl a absorption at 665 nm than the (Chl $a{\cdot}2H_2O)_n$ absorption at 743 nm (Figure 5b). The enhancement of the excitation spectral intensity in the vicinity of 619 nm relative to the optical density at corresponding wavelengths also appears to be noteworthy. The biphasic fluorescence decay of (Chl $a{\cdot}2H_2O)_n$, shown in Figure 6b,c, suggests the presence of more than one decay mechanism. A comparison of the fluorescence data in Figure 6,b and c, further indicates that, as the temperature is raised from 90 K to room temperature, the lifetime of (Chl $a{\cdot}2H_2O)_n$ fluorescence is reduced by a factor of more than 10. By contrast the monomeric Chl a fluorescence

(45) M. Kusonoki, manuscript in preparation.

(46) F. K. Fong, "Theory of Molecular Relaxation", Wiley Interscience, New York, 1975, Chapter 5.

lifetime varies from 5 ns at 294 K to 8 ns at 90 K (see Figure 6d–g), in agreement with Terenin's earlier work.[40]

The (Chl $a{\cdot}2H_2O)_n$–water photoreaction was described by a kinetic scheme that includes a two-photon mechanism.[47] The oscillations in the delayed fluorescence decay manifest[48-50] the existence of a feedback mechanism involving a decaying system that leads to the observed delayed fluorescence. The pronounced temperature and solvent effects observed in Figures 7–9 suggest that the observed oscillatory delayed-fluorescence decay may arise from hydration relaxation effects attending Chl *a*–water photoexcitation. The 77-K quench-cooling results in Figure 8 closely resemble those observed at room temperature (Figure 7). The similarity between these observations in spite of the greatly different temperatures implies that the room-temperature Chl *a* hydration effects are apparently frozen in on sample quench cooling to 77 K. The feedback mechanism responsible for the oscillatory delayed fluorescence could conceivably be given by a cyclic scheme generically related to that discussed by Hirniak[51] and Nitzan and Ross,[52] although the large amplitudes of the oscillations are not easily accounted for by the description of an incoherent kinetic system.

A linear flux dependence for the delayed fluorescence was obtained (see inset, Figure 9). Observables originating directly from excited states of the chromophore follow a relationship in which one-photon and two-photon mechanisms yield linear and quadratic flux dependences,[53] respectively. In the case of observables associated with reaction intermediates, such as Chl $a^{+\cdot}$, which may undergo bimolecular recombination in back-decay, semilinear[54] and linear flux dependences are respectively obtained for one-photon and two-photon mechanisms.[47] The delayed fluorescence predominantly originates from monomeric hydrated Chl *a*, as evidenced by the fact that the spectral distribution of the delayed fluorescence is primarily that attributable to monomeric Chl *a* fluorescence (shown in the inset of Figure 7). From a comparison of the data shown in Figure 7 it is clear that the delayed fluorescence measured at 230 ns after photoexcitation differs from the prompt fluorescence. The intensity of the long-wavelength band at 747 nm assigned to (Chl $a{\cdot}2H_2O)_n$ is significantly diminished relative to that of monomeric Chl *a* fluorescence at 670 nm. The results in Figure 9 indicate that delayed fluorescence is not obtained in ether/*n*-propanol solutions of monomeric Chl *a*, in which the chlorophyll is not complexed with water. We accordingly attribute the oscillatory fluorescent process to a charge-transfer and recombination mechanism involving the Chl *a* molecule as electron donor and water molecules of hydration as electron acceptor. Assuming further that the delayed fluorescence results from such a charge recombination mechanism, we conclude that the linear flux dependence observed in Figure 7 unequivocally supports a one-photon mechanism for the oscillatory process. It has been noted above that a reversible, light-induced ESR signal for monomeric Chl *a* radical cation is evidently not obtained independent from the dissociation equilibrium in reaction 1.

The observations of photochemical oscillations (Figures 7–9) and light-induced chlorophyll radical cation ESR signals (Figures 1–4) in the 10^{-7}–10^{-6}- and 10^{-1}–10-s time domains suggest the occurrence of two entirely different, temporally separated reaction sequences, respectively, attributable to the photoexcitation of the monomeric and aggregated hydrated Chl *a*. The reaction sequences evidently occur only when the chlorophyll is in the presence of excess water. The experimental effects obtained in this work provide comparison and contrast with corresponding effects in plant photosynthesis. Delayed fluorescence phenomena at times greater than 6 μs in chloroplast extracts[55-58] and solution[59,60] have been the subject of several earlier studies. In the present work no long-lived luminescence at times greater than ~1 μs has been observed. Van Best and Duysens[57] recently reported the observation of submicrosecond delayed fluorescence under aerobic and anaerobic conditions. The monophasic anaerobic delayed fluorescene reported by these workers is not characterized by an oscillatory behavior. It has a 0.9-μs half-life, approximately similar to the corresponding lifetime, 0.6 μs, observed for the room-temperature and quench-cooled chemiluminescence reported in the present work. No flux dependence data are available for the submicrosecond delayed fluorescence component observed in chloroplasts. Jursinic and Govindjee[56] reported a linear flux dependence for the 60-μs delayed fluorescence component in a flux range identical with that given in the inset of Figure 9. The rapid (10^{-12}–10^{-9} s) P680 reaction cycle involving pheophytin[61] as electron acceptor preceeds the slower (10^{-6}–10^{-3} s) reaction sequence culminating in the reduction of $P680^+$ by electrons from water splitting[62] and electron flow between P680 and P700.

The sharp contrast in the optical and photochemical properties of (Chl $a{\cdot}H_2O)_2$,[34] (Chl $a{\cdot}2H_2O)_n$, monomeric hydrated Chl *a*, and Chl *a* not complexed with water underscores the critical dependence of these properties on the state of Chl *a* aggregation and complexation, providing the rationale for proposing different[4-7] stereospecific Chl *a*–H_2O aggregates as models to account for the dramatic differences in the properties of P680 and P700. Significantly, of the Chl *a* complexes investigated in the present work, only (Chl $a{\cdot}2H_2O)_{n\geq 2}$ demonstrates the ability to undergo, in the presence of water, the catalytic cycle of photooxidation and dark reduction. The photocatalytic properties, as well as the observed short lifetimes and low quantum efficiencies of (Chl $a{\cdot}2H_2O)_n$ fluorescence, are generically compatible with the optical and photocatalytic properties ascribed to P680. The one-photon mechanism of monomeric Chl *a* hydrate is shown in the present investigation to result in comparatively strong prompt fluorescence and delayed fluorescence instead of photooxidation of the chlorophyll. Likewise, prompt and delayed fluorescences observed in vivo are commonly recognized as having resulted from one-photon mechanisms, properties of photochemically inactive, light-harvesting Chl *a* associated with P680.

Of course, a closer comparison of the Chl *a* photon mechanisms in vitro and in vivo requires a consideration of the effects of reactive or catalytic components complementary to the intrinsic properties of chlorophyll photoreactions with water. The oscillations in the delayed fluorescence may be indicative of feedback mechanisms involving degenerate electronic shuttling states (required[62] for the observation of these oscillations) not obtained in the in vivo system. The production and decay of (Chl $a{\cdot}2H_2O)_n^{+\cdot}$ in the in vitro photocatalytic cycle occurs on a time scale five orders of magnitude slower than the P680 reaction cycle.[63] These differences could conceivably be due to the fact that the in vivo Chl *a* photoreaction with water involves additional mechanisms, notably the Mn ap-

(47) L. Galloway, J. Roettger, ,D. R. Fruge, and F. K. Fong, *J. Am. Chem. Soc.*, **100**, 4635 (1978).
(48) P. Glansdorff and I. Prigogine, "Thermodynamic Theory of Structure, Stability and Fluctuations", Interscience, New York (1971).
(49) G. Nicolis, *Adv. Chem. Phys.*, **19**, 209 (1971).
(50) P. J. Ortoleva and J. Ross, *J. Chem. Phys.*, **55**, 4378 (1971); **56**, 287 (1972); **56**, 293 (1972); **56**, 4397 (1972).
(51) J. Hirniak, *Z. Phys. Chem.*, **75**, 675 (1911).
(52) A. Nitzan and J. Ross, *J. Chem. Phys.*, **59**, 241 (1973).
(53) J. C. Wright, *Top. Appl. Phys.*, **15**, 239 (1976).
(54) J. J. McBrady and R. Livigston, *J. Phys. Colloid Chem.*, **52**, 662 (1948).
(55) H. Hardt and S. Malkin, *Photochem. Photobiol.*, **17**, 433 (1973).
(56) P. Jursinic and Govindjee, *Photochem. Photobiol.*, **26**, 617 (1977); P. Jursinic, Govindjee, and C. A. Wraight, *ibid.*, **27**, 61 (1978).
(57) J. A. Van Best and L. N. M. Duysens, *Biochim. Biophys. Acta*, **459**, 187 (1977).
(58) G. Renger, H. J. Eckert, and H. E. Buchwald, *FEBS Lett.*, **90**, 10 (1978).
(59) A. A. Krasnovsky, Jr. and F. F. Litvin, *Photochem. Photobiol.*, **20**, 133 (1974).
(60) C. A. Parker and T. A. Joyce, *Photochem. Photobiol.*, **4**, 395 (1967).
(61) V. V. Klimov, A. V. Klevanik, V. A. Shivalov, and A. A. Krasnovsky, *FEBS Lett.*, **82**, 183 (1977); A. V. Klevanik, V. V. Klimov, V. A. Shuvalov, A. A. Krasnovsky, *Dokl. Acad. Nauk S.S.S.R.*, **236**, 241 (1977); V. V. Klimov, S. I. Allakhverdiev, V. Z. Pashchenco, *ibid.*, **242**, 1204 (1978).
(62) M. Kusunoki and F. K. Fong, *Phys. Rev. Lett.*, submitted for publication.
(63) M. Glaser, Ch. Wolf, G. Renger, *Z. Naturforsch., C*, **31**, 712 (1976); J. A. Van Best, P. Mathis, *Biochim. Biophys. Acta*, **503**, 178 (1978); A. Sonneveld, H. Rademaker, and L. N. M. Duysens, *Biochim. Biophys. Acta*, **548**, 536 (1979).

paratus for oxygen evolution and the ferredoxin intermediate pathway for CO_2 reduction. The catalytic process needed for oxygen evolution from water splitting, the possible role of two-photon mechanisms in photosynthesis,[7,47] and the effects of pheophytin and ferredoxin in mediating CO_2 reduction by hydrogen from water splitting are the subject of investigations in succeeding papers of this series.

Acknowledgment. The work reported in this paper was supported by the Basic Research Division of the Gas Research Institute.

Elementary Reconstitution of the Water Splitting Light Reaction in Photosynthesis. 2. Optical Double Resonance Study of (Chl a·$2H_2O$)$_n$ Two-Photon Interactions in Nonpolar Solutions

A. J. Alfano and F. K. Fong*

Contribution from the Department of Chemistry, Purdue University, West Lafayette, Indiana 47907. *Received October 14, 1981*

Abstract: Two-photon interactions of (Chl a·$2H_2O$)$_n$ in deaerated 1:1 n-pentane–methylcyclohexane solutions are investigated by fluorescence quenching measurements obtained by using time-resolved optical methods. The Chl a triplet state is populated by excitation with a modulated laser beam. The decay of the triplet population is monitored by measuring the quenching of Chl a fluorescence excited by a CW laser beam. The reliability of instrumental response in the dual-excitation fluorescence experiments is ensured by electronic simulations by using a red-light emitting diode simultaneously driven by a 52-Hz waveform and a weaker DC input. Flux dependence measurements are analyzed in terms of the steady-state population of the first excited singlet, S_1, under illumination by both lasers and of the flux density of the modulated laser beam. Experimental criteria are given for identifying the biphotonic mechanism responsible for the observed effects. The rationale for establishing singlet–triplet fusion as the mechanism underlying the observed behavior is provided. The possible significance of the two-photon mechanism in the Chl a water splitting reaction relative to the stereospecific interactions in hydrated Chl a aggregation is discussed.

The interest in the study of in vitro chlorophyll a photoreaction[1-9] has centered on the redox reactivity of the chlorophyll in red light, a property that underscores the remarkable ability of Chl a to transform sunlight into stored chemical energy in photosynthesis. Both metal[3-7] and semiconductor[1,2,8,9] materials have been used as electrodes for Chl a films in photoelectrochemical investigations. The experimental observations are describable in terms of Chl a photoredox reactions with the ambient electrolyte and/or the electrode material. Miyasaka et al. reported[8,9] the observation of photoanodic currents by using SnO_2 as electrode. Their results suggest the direct transfer of electrons from the chlorophyll to the conduction band of SnO_2, compatible with earlier work[1,2] and interpretation.[10,11] By contrast the currents generated by metal-based Chl a multilayers in the presence of water are photocathodic,[3-7] leading to H_2 and O_2 evolution from water splitting.[12-14] The enhancement of Pt/Chl a–H_2O photocathodic action on decreasing the electrolyte pH was observed by several workers[5,15] whose interpretations support a cyclic sequence[13] of Chl a photooxidation and subsequent reduction. The underlying photon mechanisms are of interest. The excitation of monomeric hydrated Chl a, leading to delayed fluorescence instead of photooxidation of the chlorophyll, was attributed to a one-photon process.[16] A one-photon mechanism was proposed for electron transfer from Chl a to the semiconductor electrode, whereas the Chl a water splitting reaction was interpreted in terms of a biphotonic process.[13] In this connection the possible involvement of a two-photon mechanism in the primary light reaction in plant photosynthesis was considered.[5,13] One plausible mechanism is singlet–triplet fusion resulting from annihilation,[17] through Förster energy transfer,[18] of the S_1 state of one Chl a molecule by the T_1 state of a second Chl a molecule.[19] In this work we investigate the possible origins for observations by several authors of biphotonic Chl a effects.[13,20,21]

Steady-state analyses[13,14] of Chl a photon mechanisms do not lend themselves to detailed molecular interpretations. Accordingly, we employ the time-resolved fluorescence quenching experiment designed previously in this laboratory for the delineation of Chl a photon mechanisms.[21] In this experiment optical double-resonance techniques are used. The Chl a triplet state is populated by means of a modulated laser beam. The decay of the triplet population is monitored by measuring the quenching of fluores-

(1) H. Tributsch and M. Calvin, *Photochem. Photobiol.*, **14**, 94 (1971).
(2) H. Tributsch, *Photochem. Photobiol.*, **16**, 261 (1972).
(3) F. K. Fong and N. Winograd, *J. Am. Chem. Soc.*, **98**, 2287 (1976).
(4) F. Takahashi and R. Kikuchi, *Biophys. Biochim. Acta*, **430**, 430 (1976).
(5) F. K. Fong, J. S. Polles, L. Galloway, and D. R. Fruge, *J. Am. Chem. Soc.*, **99**, 5802 (1977).
(6) J. G. Villar, *J. Bioenerg. Biomembr.*, **8**, 199 (1976).
(7) L. M. Fetterman, L. Galloway, N. Winograd, and F. K. Fong, *J. Am. Chem. Soc.*, **99**, 653 (1977).
(8) T. Miyasaka, T. Watanabe, A. Fujishima, and K. Honda, *J. Am. Chem. Soc.*, **100**, 6657 (1978).
(9) T. Miyasaka, T. Watanabe, A. Fujishima, and K. Honda, *Nature (London)*, **277**, 638 (1979).
(10) R. Memming, *Photochem. Photobiol.*, **16**, 325 (1972).
(11) H. Kuhn, *Naturwissenschaften*, **54**, 429 (1967).
(12) F. K. Fong and L. Galloway, *J. Am. Chem. Soc.*, **100**, 3594 (1978).
(13) L. Galloway, J. Roettger, D. R. Fruge, and F. K. Fong, *J. Am. Chem. Soc.*, **100**, 4635 (1978).
(14) T. Watanabe and K. Honda, *J. Am. Chem. Soc.*, **102**, 370 (1980).
(15) T. Miyasaka and K. Honda, *Surface Sci.*, in press.
(16) F. K. Fong, L. Galloway, T. G. Matthews, F. E. Lytle, A. J. Hoff, and F. A. Brinkman, *J. Am. Chem. Soc.*, preceding paper in this issue.
(17) F. K. Fong, *Proc. Natl. Acad. Sci. U.S.A.*, **71**, 3692 (1974).
(18) Th. Förster, *Ann. Phys.*, **2**, 551 (1948).
(19) T. S. Rahman and R. S. Knox, *Phys. Status Solidi B*, **58**, 715 (1973).
(20) A. F. Janzen and J. R. Bolton, *J. Am. Chem. Soc.*, **101**, 6342 (1979).
(21) E. R. Menzel, *Chem. Phys. Lett.*, **26**, 45 (1974).

0002-7863/82/1504-2767$01.25/0